Available online at www.sciencedirect.com

SciVerse ScienceDirect

Ceramics International 38 (2012) 5931–5939

CERAMICS INTERNATIONAL

www.elsevier.com/locate/ceramint

Elastic properties and damping behavior of alumina–zirconia composites at room temperature

W. Pabst [a,*], E. Gregorová [a], D. Malangré [b], J. Hostaša [a]

[a] Department of Glass and Ceramics, Institute of Chemical Technology, Prague, Technická 5, 166 28 Prague 6, Czech Republic

[b] Department of Geosciences (Applied Mineralogy), Faculty of Mathematics and Natural Sciences, Eberhardt-Karls-Universität Tübingen, Wilhelmstrasse 56, 72074 Tübingen, Germany

Received 16 March 2012; received in revised form 13 April 2012; accepted 14 April 2012
Available online 21 April 2012

Abstract

Alumina–zirconia composite ceramics (AZ composites) have been prepared in the whole range of compositions from pure alumina to zirconia (in steps of 10 vol.%) by slip casting, followed by sintering at 1350 °C and microstructural characterization via the Archimedes method (relative densities 0.93–0.99). Young's modulus has been measured at room temperature via the impulse excitation technique (IET) and, after appropriate porosity correction (linear, power-law, exponential), found to be in good agreement with the Hashin–Shtrikman bounds. The damping factor (internal friction), which has been measured for dense AZ composites (also via IET at room temperature), is found to increase with increasing zirconia content. Damping factors measured for porous AZ composites with porosities 25–71%, prepared with corn starch as a pore former, have been found to depend only slightly on porosity, unless the porosities are extremely high (>70%). At these porosities, however, where the Young's moduli approach zero, the damping factors exhibit a steep increase.

Keywords: Alumina; Zirconia; Alumina–zirconia composites; Elastic moduli (Young's modulus); Mechanical damping; Porous ceramics (porosity)

1. Introduction

Alumina–zirconia composites are widely used in many fields of application due to their outstanding mechanical properties, in particular high strength and fracture toughness [1–3]. Therefore the elastic properties of alumina–zirconia composites have been of general interest for more than three decades now. In spite of many elastic modulus data scattered in the literature, however, there seems to be no work available in which these data have been measured systematically in the whole range of compositions and analyzed in terms of the rigorous micromechanical bounds [4]. This paper intends to fill this gap, at least for the Young's modulus. Moreover, internal friction is investigated in terms of the damping factor Q^{-1} (specific damping), measured via the impulse excitation technique [5,6]. In contrast to the elastic constants, the internal friction is a measure of energy dissipation during vibration or impact and can provide important additional information on material performance, especially for strongly dissipative materials and in damage-related processes. While the temperature dependence of damping has been reported for several ceramics, including alumina [5], zirconia [5,7], silicon carbide [8,9], silicon nitride [9], zinc oxide [10], lead zirconate–titanate [11], ternary carbides (MAX phases) [12] and certain alumina–zirconia composites and laminates [13,14], a systematic work covering the whole range of alumina–zirconia composite compositions at room temperature is not available so far. In particular, not much is known concerning the dependence of damping or internal friction in composite ceramics on composition and porosity. In this paper we present broad evidence for the view that – despite the fact that internal friction and damping is principally dependent on the porosity and possibly other microstructural details (pore size, pore shape and pore space characteristics) [15–17] – the influence of porosity is comparatively low, unless a critical porosity level is approached. Although external causes and singular defects inside the material, such as cracks, may occasionally lead to unusually high damping factors (usually

* Corresponding author.
E-mail address: pabstw@vscht.cz (W. Pabst).

0272-8842/$36.00
http://dx.doi.org/10.1016/j.ceramint.2012.04.045

accompanied by very low elastic moduli), Q^{-1} data corresponding to undamaged samples without external friction sources are shown to exhibit a clear and distinct dependence on composition in the case of alumina–zirconia composites. After presenting theoretical and experimental preliminaries, Young's modulus and damping data will be presented, and the correlation between the porosity dependence of these two quantities will be highlighted.

2. Theoretical

The elastic moduli of two-phase composites are bounded from above and below by the Paul bounds [18] (the upper and lower Paul bounds are also called Voigt and Reuss bounds, respectively) [19]. For the shear and bulk moduli G and K these upper and lower bounds are represented by the volume-weighted arithmetic and harmonic mean, respectively:

$$M_P^+ = \phi_1 M_1 + \phi_2 M_2, \tag{1}$$

$$M_P^- = \frac{M_1 M_2}{\phi_1 M_2 + \phi_2 M_1}, \tag{2}$$

where M_P^+ and M_P^- denote the upper and Paul bounds, respectively, of the modulus in question, ϕ_i the volume fractions of the two phases and M_i the phase moduli. For the Young's modulus (tensile modulus) E, only the lower bound is strictly given by Eq. (2), while the upper bound must principally be calculated using the (upper bounds of the) bulk and shear moduli via the elasticity standard relation [20]

$$E^+ = \frac{9K^+G^+}{3K^+ + G^+}. \tag{3}$$

Only in the special case of equal Poisson ratios of both phases the upper bound for the Young's modulus is rigorously given by the (volume-weighted) arithmetic mean, Eq. (1). Note in passing that for the effective Poisson ratio no rigorous bounds are known, except for the universally valid thermodynamic stability bound $-1 < \nu < 0.5$ [21].

While the Paul bounds are valid for arbitrary microstructures, more restrictive bounds can be given in the case of isotropic microstructures, the Hashin–Shtrikman bounds [22]. For the shear and bulk moduli of two-phase composites with $K_1 > K_2$ and $G_1 > G_2$ the Hashin–Shtrikman upper bounds are

$$G_{HS}^+ = G_1 + \left[\frac{1}{G_2 - G_1} + \phi_2 \cdot \frac{6(K_1 + 2G_1)}{5G_1(3K_1 + 4G_1)}\right]^{-1} \cdot \phi_2, \tag{4}$$

$$K_{HS}^+ = K_1 + \left[\frac{1}{K_2 - K_1} + \phi_1 \cdot \frac{3}{3K_1 + 4G_1}\right]^{-1} \cdot \phi_2, \tag{5}$$

and the corresponding lower bounds are obtained by switching the indices [4,23]. As before, the Hashin–Shtrikman bounds for the Young's modulus can be calculated using the elasticity standard relation (Eq. (3)), and its equivalent for the lower bounds.

Porous materials can be considered as a special case of two-phase composites, for which the elastic moduli of one phase (the void phase) are zero, e.g. $E_2 = 0$. In this case it is common practice to introduce relative elastic moduli M_r via the relation

$$M_r = \frac{M}{M_0}, \tag{6}$$

where M is the effective modulus of the porous material and M_0 the modulus of the solid phase (or phase mixture). In particular, in terms of the porosity (volume fraction of pores) $\phi(\equiv\phi_2)$ the upper Paul and Hashin–Shtrikman bounds of the Young's modulus are [23]

$$E_r = 1 - \phi \tag{7}$$

and

$$E_r = \frac{1 - \phi}{1 + \phi}, \tag{8}$$

respectively (the lower bounds are identically zero in this case). Any admissible relation for the porosity dependence of the Young's modulus must obey these bounds. The simplest of these is the linear approximation (also called dilute or non-interaction approximation) [24]

$$E_r = 1 - 2\phi, \tag{9}$$

which represents the exact solution for a spherical void in an infinite medium and can be assumed to be valid for low porosities. In the case of higher porosities nonlinear relations have to be used. The most succesful of these are the power-law relation [25]

$$E_r = (1 - \phi)^2, \tag{10}$$

the exponential relation [26]

$$E_r = \exp\left(\frac{-2\phi}{1 - \phi}\right), \tag{11}$$

and the sigmoidal average of the Hashin–Shtrikman bounds [27]. These relations can be used to estimate the effective Young's modulus E of a porous material or to extrapolate measured values of E in order to obtain the Young's modulus of the dense (i.e. pore-free) solid phase (or phase mixture). The latter possibility will be exploited in this paper.

It is well known that the elastic constants of ceramics and composites can be measured via static or dynamic measuring techniques. The former provide isothermal elastic constants, the latter adiabatic (isentropic) ones [23]. For reasons of simplicity the latter, dynamic measuring techniques, especially the resonant frequency technique [28,29] and the impulse excitation technique [5–7,9,10], have become more and more popular during the last 15 years. It should be emphasized, however, that all aforementioned relations hold for both types of elastic moduli. Moreover, in the case of alumina and zirconia the difference between the isothermal (static) and adiabatic (dynamic) elastic constants is very small: an estimate yields a difference in the Young's moduli of only 0.3% [23], which is usually smaller than the precision of experimental measurements and certainly negligible with respect to sample preparation scatter.

Apart from the elastic moduli, which are obtained via the resonant frequencies, the impulse excitation technique allows the determination of the damping behavior of materials [5,7,9,10]. This feature is analyzed by evaluating the exponential decay of the signal amplitude for freely vibrating samples suspended exactly at the nodes (to ensure greatest possible absence of external friction). Sufficiently small-amplitude, damped flexural vibrations of a long beam or rod with internal friction can be described via the equation

$$x(t) = x_0 \cdot \exp(-kt) \cdot \cos(\omega t + \theta), \tag{12}$$

where x is the displacement, t time, x_0 the initial amplitude, k the amplitude decay constant (inverse characteristic decay time), ω the angular frequency (related to the fundamental resonant frequency $f = \omega/2\pi$) and θ the phase lag. The amplitude decay constant k is characteristic of the (freely vibrating) body, while the damping factor Q^{-1} (also called specific damping, internal friction or simply damping [9,10,14]), defined as

$$Q^{-1} = \frac{k}{\pi f}, \tag{13}$$

is a dimensionless quantity characterizing internal friction of the material. Theory predicts enhanced internal friction and thus damping in more defective structures, the main source being elastic dipoles formed e.g. by the coupling of oxygen vacancies and associated yttrium substitutional ions in doped zirconia [30]. Therefore damping should be expected to be more significant in doped zirconia than in pure alumina for example.

3. Experimental

Widely used commercial submicron alumina (α-Al_2O_3) and zirconia (t-ZrO_2 with 3 mol.% Y_2O_3) powders have been used in this work for the preparation of dense and porous alumina–zirconia composites (AZ composites) by traditional slip casting (in plaster molds) and starch consolidation casting (in metal molds), respectively.

Dense AZ composites were prepared in the whole range of compositions from pure alumina to zirconia in steps of 10 vol.% (assuming theoretical densities of 4.0 and 6.1 g/cm^3 for alumina and zirconia, respectively) by traditional slip casting using Taimicron TM-DAR alumina (Taimei Chemicals, Japan; low-temperature sinterable alumina with a median particle size of 0.1–0.2 μm and a specific surface of 14.5 m^2/g) and TZ-3YE zirconia (Tosoh, Japan; median particle size approx. 0.2 μm, crystallite size 28–40 nm, specific surface area approx. 16 m^2/g). In the sequel the compositions labeled A100Z0, A90Z10, A80Z20, etc. denote AZ composites with zirconia volume fractions of 0, 0.1, 0.2, etc.

Porous AZ composites were prepared by starch consolidation casting using AA04 alumina (Sumitomo, Japan; median particle size approx. 0.4 μm, specific surface area approx. 4 m^2/g) and TZ-3Y zirconia (Tosoh, Japan; median particle size approx. 0.4 μm, crystallite size 28–40 nm, specific surface area approx. 16 m^2/g). Corn starch (Gustin, Dr. Oetker, Czech Republic) with a median diameter of 14 μm has been used as a fugitive pore former (and consolidating agent). Four types of composites were prepared, containing 10, 20, 30 and 40 wt.% of zirconia (labeled A90Z10, A80Z20, A70Z30 and A60Z40). Of each of these four compositions four variants with different porosities were prepared from suspensions with nominal starch contents in the range 10–50 vol.% (density of corn starch: 1.5 g/cm^3) [27].

Aqueous suspensions containing the ceramic powder mix, distilled water and deflocculant (Dolapix CE64, Zschimmer & Schwarz, Germany) in a concentration of 1 wt.% (related to the ceramic powder), were prepared by 2 h homogenization in polyethylene bottles with alumina balls on a laboratory shaker (HS260, IKA, Germany), followed by ultrasonication (UP200S, Dr. Hielscher, Germany). For the preparation of porous composites cornstarch was added. The concentrations of ceramic powders in the suspensions used were 70 wt.% for traditional slip casting (dense AZ composites) and 73–75 wt.% (lower for larger starch contents and vice versa) for starch consolidation casting (porous AZ composites). The as-prepared, ready-to-cast mixed slurries were cast into plaster or brass molds with a cylindrical cavity of internal diameters 5 mm and 7 mm and lengths of approx. 50 mm and 70 mm, respectively. Further details of the preparation processes have been given elsewhere [27]. After consolidation of the green state (body formation) and demolding the samples were dried under ambient conditions for 24 h, and then at 60, 80 and 105–110 °C until mass constancy, with a 2 h dwell at the first two temperatures. Dense AZ composites were prepared from green bodies containing the low-temperature sinterable alumina TM-DAR (without starch) by sintering at a temperature of 1350 °C, in accordance with the producers' data sheet recommendation. Porous AZ composites (from starch-containing green bodies) have been prepared by firing at 1530 °C (full sintering of the matrix) and at 1100, 1200, 1300 and 1400 °C (partial sintering of the matrix). Based on previous experience [31,32], the same standard firing schedule has been used in all cases (heating rate 2 °C/min, 2 h dwell).

The as-fired samples were characterized with respect to shrinkage by a slide caliper. Their bulk density and open porosity were determined via the Archimedes technique after 2 h boiling in water and allowing a soaking time of 24 h. The total porosity was determined based on the theoretical density of each composition, taking the density values 4.0 g/cm^3 and 6.1 g/cm^3 for the pure alumina and zirconia end members, respectively.

Young's moduli were measured on cylindrical rods via the impulse excitation technique in the flexural vibration mode using an impulse excitation instrument (RFDA 23, IMCE, Belgium) with fast Fourier transformation software. The Young's moduli were calculated via the RFDA-MF software (according to the ASTM E 1259 standard) via the equation

$$E = 1.6067 \cdot \left(\frac{L^3}{D^4}\right) \cdot (m \cdot f^2) \cdot C, \tag{14}$$

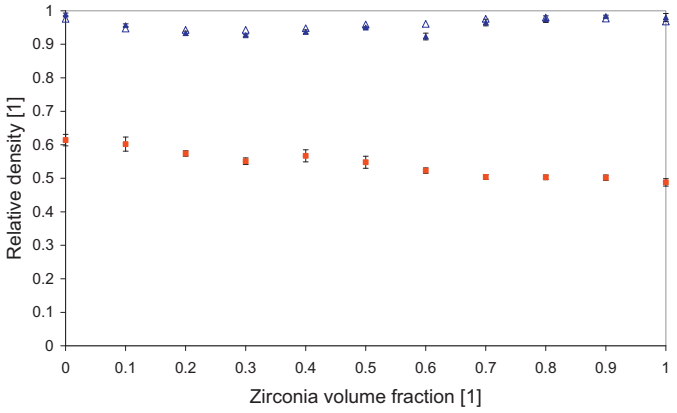

Fig. 1. Relative density of alumina–zirconia composites in the green state (full squares) and after firing at 1350 °C; data for cylindrical samples prepared in this work (full traingles) compared to data for disk-shaped samples (empty triangles) prepared in previous work [35].

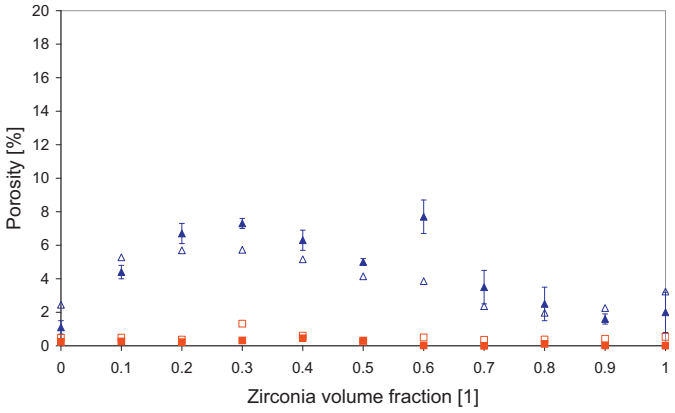

Fig. 2. Porosity (triangles: total, squares: open) of alumina–zirconia composites after firing at 1350 °C; data for cylindrical samples prepared in this work (full symbols) compared to data for disk-shaped samples (empty diamonds) prepared in previous work [35].

where L is the rod length, D the rod diameter, m the mass of the rod, f the fundamental resonant frequency for flexural vibrations and C a correction factor dependent on the aspect ratio of the rod and the Poisson ratio of the material [6,33].

The damping factor (specific damping, internal friction) is calculated from the measured resonant frequency and the amplitude decay constant k (see Eq. (13)).

4. Results and discussion

Fig. 1 shows the relative density of alumina–zirconia composites in the green state and after firing at 1350 °C in dependence of the zirconia volume fraction. It is evident that the relative green density decreases in an approximately linear manner from a value of approx. 0.61–0.49 for the pure alumina and zirconia end members, see Table 1. This behavior is typical and is obviously related to the fact that the volume fraction of zirconia in the 70 wt.% suspensions is much smaller (27.7 vol.%) than for alumina (36.8 vol.%). As a consequence, the packing fraction of alumina is close to that of random packing (more precisely, between loose and dense random packing [34]), whereas that of zirconia is much lower. The reasons for this different behavior are of course quite complex (particle shape, surface, size distributions, and interactions) and a thorough discussion would be beyond the scope of this paper. Anyway, irrespective of the reasons for this difference and its tentative explanations, it is a fact that for the powders used here this simple (approximately linear) dependence exists. After firing, however, the relative density exhibits a characteristic change: there is a minimum in the relative density (and a corresponding maximum in the total porosity, see Fig. 2) for a zirconia content of approx. 30 vol.% (corresponding to A70Z30 composites), a result that confirms previous findings with differently shaped samples [35]. Evidently, this is a consequence of constrained sintering of mixed powders [36], and it may be hypothesized that the 30 vol.% value corresponds to the percolation threshold of zirconia in the alumina matrix. During cooling from the sintering temperature the zirconia grains, which have at this concentration just attained the percolation threshold and thus form a contact skeleton in the grainy alumina matrix (made from easily sinterable alumina powder), tend to shrink slightly more than the matrix (because of the higher thermal expansion coefficient [37]), thereby loosing contact and leaving void spaces in the composite. We emphasize, however, that this thermal mismatch effect is not very large: the relative density values range from 0.99 down to approx. 0.93 (corresponding to total porosities of maximally 7%). Higher densities could of course be obtained by optimizing the

Table 1
Microstructural characteristics of alumina–zirconia composites (Taimicron TM-DAR and Tosoh TZ-3YE) after firing at 1350 °C (rate 2 °C/min, 2 h dwell).

Composite type	Theoretical density (g/cm^3)	Relative green density (%)	Shrinkage (%)	Bulk density (g/cm^3)	Relative density after firing (%)	Total porosity (%)	Open porosity (%)
A100Z0	4.00	61.4 ± 1.7	14.4 ± 0.7	3.95 ± 0.02	98.9	1.1 ± 0.4	0.23
A90Z10	4.21	60.2 ± 2.1	14.2 ± 0.8	4.03 ± 0.01	95.7	4.4 ± 0.4	0.26
A80Z20	4.42	57.4 ± 0.8	14.6 ± 0.3	4.12 ± 0.03	93.3	6.7 ± 0.6	0.22
A70Z30	4.63	55.1 ± 1.0	15.7 ± 0.5	4.30 ± 0.01	92.7	7.3 ± 0.3	0.32
A60Z40	4.84	56.7 ± 1.8	15.0 ± 0.5	4.53 ± 0.03	93.7	6.3 ± 0.6	0.45
A50Z50	5.05	54.8 ± 1.8	15.6 ± 0.4	4.80 ± 0.01	95.0	5.0 ± 0.2	0.31
A40Z60	5.26	52.3 ± 0.8	17.2 ± 0.3	4.85 ± 0.05	92.3	7.7 ± 1.0	0.02
A30Z70	5.47	50.4 ± 0.7	18.8 ± 0.1	5.28 ± 0.05	96.5	3.5 ± 1.0	0
A20Z80	5.68	50.3 ± 0.7	19.8 ± 0.2	5.54 ± 0.06	97.5	2.5 ± 1.0	0.11
A10Z90	5.89	50.2 ± 0.8	20.3 ± 0.2	5.80 ± 0.01	98.4	1.6 ± 0.3	0.02
A0Z100	6.10	48.8 ± 1.1	20.7 ± 0.2	5.98 ± 0.07	98.0	2.0 ± 1.2	0.01

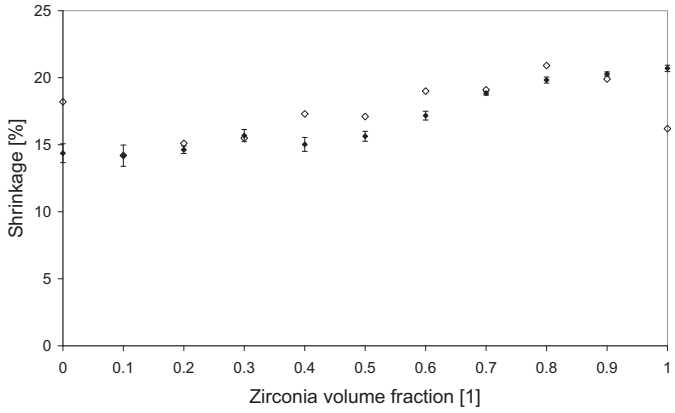

Fig. 3. Shrinkage of alumina–zirconia composites after firing at 1350 °C; data for cylindrical samples prepared in this work (full diamonds) compared to data for disk-shaped samples (empty diamonds) prepared in previous work [35].

sintering schedule for each composition, but this was not intended in the present paper; on the contrary, special care has been taken to keep the processing conditions identical for all composite samples prepared without pore-forming agents. From Fig. 2 it is evident that for all compositions the porosity is essentially closed (open porosities <0.5%, see Table 1). We note in passing that the highest bulk densities measured for our pure alumina and zirconia end members were 3.98 and 6.08 g/cm^3, respectively, indicating that the theoretical density values of 4.00 and 6.10 g/cm^3 must be considered realistic. From Fig. 3 it can be seen that shrinkage after firing is between approx. 14% for alumina and approx. 21% for zirconia. All composites exhibit shrinkage values in between these two extremes, exhibiting a trend of increasing shrinkage with increasing zirconia volume fraction.

Young's moduli of dense alumina–zirconia composites can be obtained by extrapolating the measured values (for composites with up to 7–8% porosity), using one of the aforementioned modulus–porosity relations. Table 2 shows the extrapolated values obtained using the linear approximation (Eq. (9)), the power law (Eq. (10)), and the exponential relation (Eq. (11)). It is evident that – for the rather low porosities in question – any of these corrections can be used. (For higher porosities the exponential relation, which can be seen to be intermediate between the linear and the power-law correction, is usually preferred [38,39], because it has turned out to be the most realistic relation for most microstructures [40,41]). Fig. 4 shows the extrapolated Young's moduli in comparison to the Paul (Voigt–Reuss) bounds and the Hashin–Shtrikman bounds. For the construction of these bounds the extrapolated Young's moduli of the pure alumina and zirconia end members have been used (i.e. 413.6 and 223.1 GPa from Table 2), the Poisson ratios have been taken from the literature (0.23 and 0.29, respectively [23]) and the shear and bulk moduli have been calculated using elasticity standard relations [20], resulting in shear moduli of 168.1 and 86.5 GPa and bulk moduli of 255.3 and 177.1 GPa for alumina and zirconia, respectively. As expected, the effective Young's moduli of the alumina–zirconia composites come to lie nicely within the Paul bounds and are rather precisely predicted via the Hashin–Shtrikman bounds. Note that the extrapolated Young's moduli reported here are close to, but systematically slightly higher than, literature data published for alumina–zirconia composites made from other commercial powders [23,42,43]. This discrepancy cannot be explained by the fact that other authors use other measuring techniques because all these data were obtained by dynamical techniques and a simple estimate has shown that in the alumina–zirconia system even static measurements can account only for decrease in the Young's modulus of approx. 0.3% [23], a value which would be completely negligible here. Therefore we attribute the slight discrepancy to the literature data primarily to the absence of a porosity correction in the previous works cited. For practical purposes and later reference, and in order to achieve highest precision in the interpolation of Young's modulus data for dense alumina–zirconia composites in the whole range of compositions, the extrapolated values have been fitted using a third-order polynomial. The resulting practical interpolation formula is

$$E_0(\phi_Z) = 413.6 - 314.9\ \phi_Z + 239.8\ \phi_Z^2 - 116.0\ \phi_Z^3 \qquad (15)$$

Table 2
Young's moduli extrapolated to zero porosity according to the linear approximation, the power law and the exponential relation (averages of measured values for samples with residual porosity are given only for reasons of comparison; note that porosity corrections have been performed for each of the 3–5 samples of each composition type individually).

Composite type	Average of measured Young's moduli (GPa)	Young's modulus of dense composites (GPa) obtained by extrapolation according to the …			Average of the three extrapolations
		… linear relation	… power law	… exponential	
A100Z0	397.1	413.6 ± 3.5	413.5 ± 3.5	413.6 ± 3.5	413.6 ± 3.5
A90Z10	374.8	387.5 ± 6.9	386.7 ± 6.9	387.5 ± 6.9	387.2 ± 6.9
A80Z20	336.1	354.4 ± 14.4	352.4 ± 14.0	354.3 ± 14.3	353.7 ± 14.2
A70Z30	314.1	338.3 ± 7.6	336.2 ± 7.4	338.2 ± 7.5	337.6 ± 7.5
A60Z40	272.2	321.4 ± 7.6	319.9 ± 7.6	321.3 ± 7.6	320.9 ± 7.6
A50Z50	273.7	304.8 ± 8.0	301.9 ± 6.5	304.6 ± 7.8	303.8 ± 7.3
A40Z60	251.0	285.0 ± 8.2	283.0 ± 7.5	284.9 ± 8.1	286.7 ± 8.8
A30Z70	229.4	268.1 ± 5.7	267.7 ± 5.8	268.1 ± 5.7	268.0 ± 5.7
A20Z80	221.8	255.8 ± 5.5	255.6 ± 5.3	255.8 ± 5.5	255.7 ± 5.4
A10Z90	218.9	239.8 ± 5.2	239.8 ± 5.2	239.8 ± 5.2	239.8 ± 5.2
A0Z100	218.2	223.1 ± 12.2	223.0 ± 12.1	223.1 ± 12.2	223.1 ± 12.1

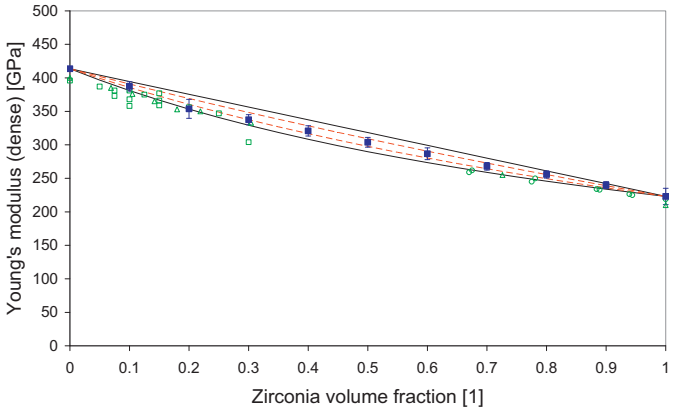

Fig. 4. Young's modulus of alumina–zirconia composites after firing at 1350 °C (full squares); compared to the Paul bounds (Voigt–Reuss bounds, full curve), the Hashin–Shtrikman bounds and literature data (empty squares [42], empty triangles [23], empty circles [43]).

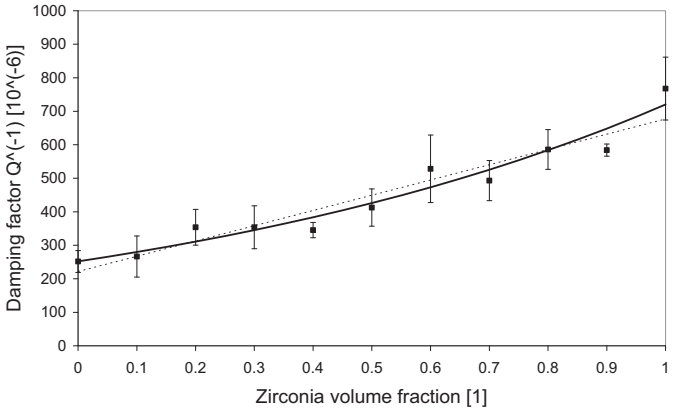

Fig. 6. Damping factor (internal friction) of dense alumina–zirconia composites after firing at 1350 °C (full squares) fitted by linear regression (dotted line, correlation coefficient 0.957) and an empirical power-law or exponential fit relation (correlation coefficient 0.971).

(fitted by nonlinear regression with a correlation coefficient of 0.999), where ϕ_Z is the zirconia volume fraction, see Fig. 5. This interpolation formula is in reasonable agreement with other similar formula, which have been published previously [23], but it is clear that at this level of precision even powder-specific influences may come into play.

Fig. 6 shows the damping factor (internal friction) of alumina–zirconia composites, as measured. Notwithstanding some scatter, there is a clear and distinct trend towards higher damping with increasing zirconia content. Q^{-1} values range from approx. 250×10^{-6} to approx. 770×10^{-6}, a range that is in good agreement with other authors' results at room temperature for alumina ($120–700 \times 10^{-6}$ reported by Roebben et al. [5]) and is of the same order of magnitude as for alumina–zirconia laminates [14] and other ceramics such as silicon nitride [5], silicon carbide [8] and certain ternary carbides (MAX phases) [8]. The damping factor of metallic materials, e.g. porous or foamed aluminum, is typically higher by one order of magnitude [15,16]. The increasing damping with increasing zirconia content in Fig. 6 is not too surprising, because the zirconia structure is a highly defective one and the magnitude of damping is related to the amount of Y^{3+} ions in the ZrO_2 lattice [7]. For alumina–zirconia composites prepared in the way described above from the aforementioned powders the depedence of the damping factor at room temperature can be described via empirical fit relations, e.g. the linear relation

$$Q^{-1} = 222 + 455.3\ \phi_Z \tag{16}$$

(fitted with correlation coefficient 0.957) or the exponential or power-law relation

$$Q^{-1} = 252 \cdot \exp(1.05\ \phi_Z) = 252 \cdot 2.849^{\phi_Z} \tag{17}$$

(fitted with correlation coefficient 0.971). It is interesting that in practice these fits yield good estimates of the damping factors of alumina–zirconia composites up to remarkably high porosities. Although it is well known that the microstructure, in particular porosity (and even pore size and shape as well as the connectivity of the pore space), certainly does have an influence on the damping behavior of ceramics [17], this influence seems to be overestimated in the literature so far.

Fig. 7 shows the porosity dependence of the damping factor for AZ composites containing from 10 to 40 vol.% zirconia (i.e. A90Z10, A80Z20, A70Z30, A60Z40). Data points with

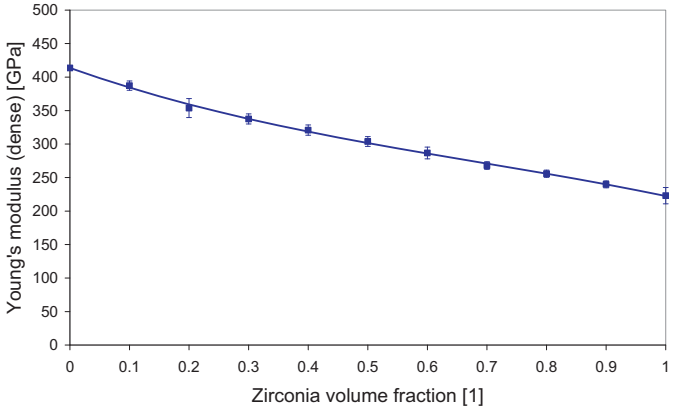

Fig. 5. Young's modulus of alumina–zirconia composites after firing at 1350 °C (full squares) fitted by a third-order polynomial (correlation coefficient 0.999).

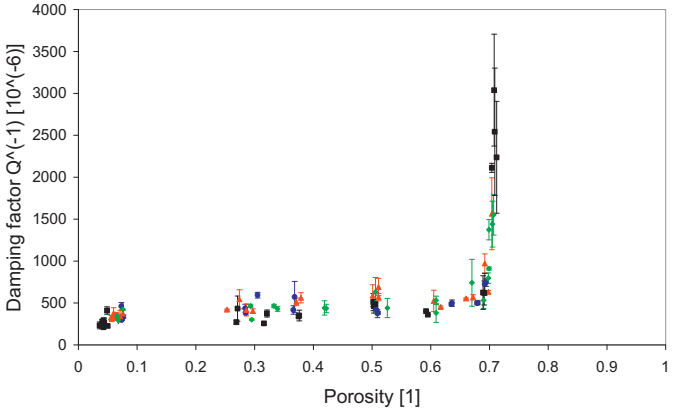

Fig. 7. Porosity dependence of the damping factor (internal friction) for alumina–zirconia composites of composition A90Z10 (squares), A80Z20 (diamonds), A70Z30 (circles) and A60Z40 (triangles).

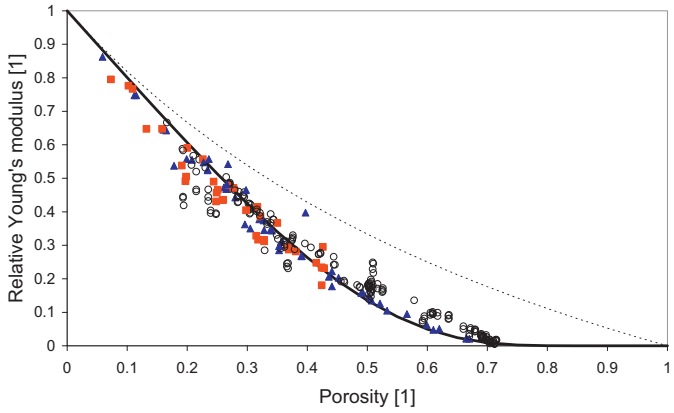

Fig. 8. Porosity dependence of the relative Young's modulus for porous ceramics prepared with starch as a pore former, fully or partially sintered; data for alumina (full triangles [44–46]), zirconia (full squares [44–46]) and alumina–zirconia composites (empty circles [27,44,46,47]) compared to the Hashin–Shtrikman upper bound (dotted curve) and the exponential prediction (full curve).

porosities below 10% refer to AZ composites prepared without pore formers (powders Taimicron TM-DAR and Tosoh TZ-3YE), whereas data points with porosities from approx. 25% to approx. 53% refer to AZ composites prepared with corn starch as a pore former and points with porosities >59% refer to partially sintered samples of the latter type (temperatures down to 1100 °C, powders Sumitomo AA04 and Tosoh TZ-3Y) [27]. It is evident, that for porosities in the wide range from around 5% up to more than 60% (!) – although there seems to be a slightly increasing trend – the influence of porosity is so small that it almost vanishes in comparison to the scatter of experimental data. At porosities >70%, however, the damping factor exhibits a steep increase. It has to be noted that these results cover a wide range of zirconia contents (10–40 vol.%), each with a very wide range of porosities (from approx. 5% to more than 70%). Concomitantly with this steep increase of the damping factor, the Young's modulus tends to zero at porosities just above 70%, see Fig. 8. It has to be emphasized the specific

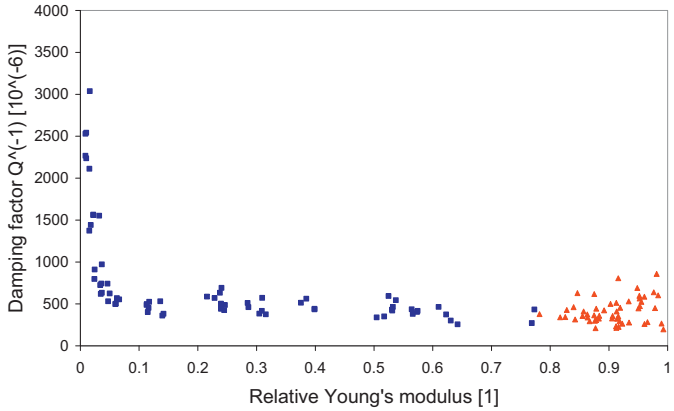

Fig. 9. Correlation between damping factor (internal friction) and relative Young's modulus for alumina–zirconia composites; relative Young's moduli: >0.77 – dense composites (triangles) in the whole range of compositions from A100Z0 to A0Z100, <0.65 – porous composites (squares) in the range from A60Z40 to A90Z10.

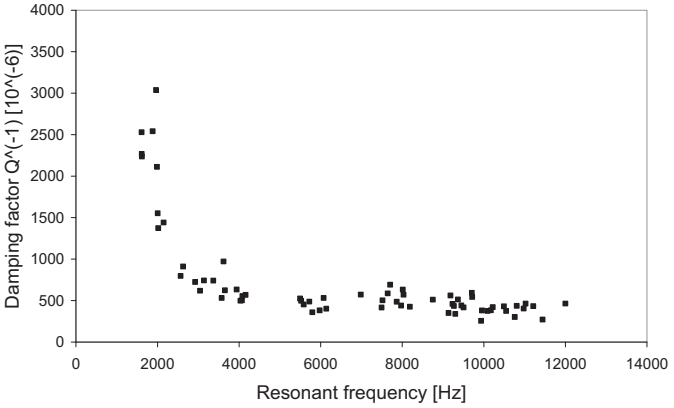

Fig. 10. Frequency dependence of the damping factor (internal friction) for porous alumina–zirconia composites with compositions in the range from A60Z40 to A90Z10.

value of 70% is not universal, but must be interpreted as a typical feature of porous ceramics prepared using pore-forming agents [27,44–47]. Fig. 9 clearly documents the correlation between the damping factor and the relative Young's modulus. It is evident that – with regard to experimental scatter – the damping factor is essentially independent of the relative Young's modulus, unless very small relative Young's moduli are attained (below 0.05). Taking into account that the relative Young's modulus is related to the resonant frequency of the material, the dependence of the damping factor on frequency can be expected to be similar. Fig. 10 shows that obviously – despite the principally hyperbolic dependence [17], cf. also Eq. (13) – there is no significant dependence of the damping factor on the resonant frequency for alumina–zirconia composites at room temperature, unless low frequencies are attained (below 3000 Hz).

5. Summary and conclusion

Alumina–zirconia composite ceramics (AZ composites) have been prepared in the whole range of compositions from pure alumina to zirconia (in steps of 10 vol.%) by slip casting from mixed suspensions. It has been found that the relative green density (packing fraction) exhibits an approximately linear decrease from approx. 0.61 for alumina to 0.49 for zirconia. After firing at 1350 °C, relative densities between 0.93 and 0.99 have been attained, with a minimum (corresponding to a total porosity of approx. 7%) for a zirconia content of 30 vol.%. Open porosity is negligible throughout (<0.5% for all compositions) and the shrinkage is between 14 and 21%, with an increasing trend with increasing zirconia volume fraction.

Young's modulus measurements were performed at room temperature via the impulse excitation technique. As expected, after appropriate correction for the influence of porosity (using the linear approximation, the power law or the exponential relation), the extrapolated Young's moduli are close to, but slightly higher than, typical literature values reported previously for more or less dense AZ composite ceramics. Using the values determined in this work for the pure alumina and

zirconia end members (413.6 and 223.1 GPa, respectively), the Young's moduli for the AZ composites come to lie within the Paul (Voigt–Reuss) bounds and are well predicted by any average of the Hashin–Shtrikman bounds. For easy reference, a third-order polynomial fit has been given for calculating effective Young's moduli of dense AZ composites prepared from the powders used (Taimicron TM-DAR and Tosoh TZ-3YE).

Also the damping factor (internal friction) has been measured for AZ composites at room temperature via the impulse excitation technique. It has been found that the damping of dense AZ composites increases with increasing zirconia content. Empirical fit equations (linear, power-law and exponential) have been given to describe this dependence. In addition to the dense samples, the damping factor was measured for porous AZ composites with zirconia contents of 10, 20, 30 and 40 vol.% prepared by starch consolidation casting with corn starch as a fugitive pore former, applying either full or partial sintering of the ceramic matrix, resulting in porosities between 25 and 71%. It has been found that, in contrast to common belief, the dependence of the damping factor on porosity is not very significant unless the porosities are extremely high (>70%). At these porosities, however, the damping factor exhibits a steep increase. At the same time the resonant frequency is low for such highly porous materials (<3000 Hz) and, concomitantly with the divergence of the damping factor, the Young's moduli approach zero.

Acknowledgements

This study is part of the project GAČR P108/12/1170 ''Porous ceramics with controlled elasticity and thermal conductivity'', supported by the Grant Agency of the Czech Republic (Grantová agentura České republiky). Support is gratefully acknowledged. The authors also thank Prof. Dr. K.G. Nickel and Dr. C. Berthold from the Department Geosciences (Applied Mineralogy) of the University Tübingen (Germany) for helpful discussions.

References

[1] W.E. Lee, W.M. Rainforth, Ceramic Microstructures – Property Control by Processing, Chapman & Hall, London, 1994, pp. 534–538.
[2] J.B. Wachtman, Mechanical Properties of Ceramics, John Wiley & Sons, New York, 1996, pp. 391–407.
[3] P.F. Becher, L.R.F. Rose, Toughening mechanisms in ceramic systems, in: M. Swain (Ed.), Structure and Properties of Ceramics, Cahn, in: R.W. Cahn, P. Haasen, E.J. Kramer (Eds.), Materials Science and Technology – A comprehensive Treatment, Wiley-VCH, Weinheim, 2005, pp. 409–461.
[4] S. Torquato, Random Heterogeneous Materials–Microstructure and Macroscopic Properties, Springer, New York, 2002, pp. 403–621.
[5] G. Roebben, B. Bollen, A. Brebels, J. van Humbeeck, O. van der Biest, Impulse excitation apparatus to measure resonant frequencies, elastic moduli, and internal friction at room and high temperature, Review of Scientific Instruments 68 (1997) 4511–4515.
[6] ASTM standard E 1876–99, Standard Test Method for Dynamic Young's Modulus, Shear Modulus, and Poisson's Ratio by Impulse Excitation of Vibration, American Society for Testing and Materials, West Conshohocken/PA, 1999.
[7] G. Roebben, B. Basu, J. Vleugels, O. van der Biest, Transformation-induced damping behaviour of Y-TZP zirconia ceramics, Journal of the European Ceramic Society 23 (2003) 481–489.
[8] A. Wolfenden, C.B. Proffitt, M. Singh, Dynamic elastic modulus and vibration damping behavior of porous silicon carbide ceramics at elevated temperatures, Journal of Materials Engineering and Performance 8 (1999) 598–600.
[9] G. Roebben, R.G. Duan, D. Sciti, O. van der Biest, Assessment of the high temperature elastic and damping properties of silicon nitrides and carbides with the impulse excitation technique, Journal of the European Ceramic Society 22 (2002) 2501–2509.
[10] A.K. Swarnakar, L. Donzel, J. Vleugels, O. van der Biest, High temperature properties of ZnO ceramics studied by the impulse excitation technique, Journal of the European Ceramic Society 29 (2009) 2991–2998.
[11] R. Fu, T.Y. Zhang, Influences of temperature and electric field on the bending strength of lead zirconate titanate ceramics, Acta Materialia 48 (2000) 1729–1740.
[12] M. Radovic, M.W. Barsoum, A. Ganguly, T. Zhen, P. Finkel, S.R. Kalidindi, E. Lara-Curzio, On the elastic properties and mechanical damping of Ti_3SiC_2, Ti_3GeC_2, $Ti_3Si_{0.5}Al_{0.5}C_2$ and Ti_2AlC in the 300–1573 K temperature range, Acta Materialia 54 (2006) 2757–2767.
[13] D. Samatowicz, O. Olszewski, T.A. Stolarski, Studies into the physical properties of a ceramic material with deposited film of lubricant, Ceramics International 22 (1996) 187–191.
[14] K. Lambrinou, T. Lauwagie, F. Chalvet, G. de Portu, N. Tassini, S. Patsias, O. Lube van der Biest, Elastic properties and damping behaviour of alumina–alumina/zirconia laminates, Journal of the European Ceramic Society 27 (2007) 1307–1311.
[15] C.S. Liu, Z.G. Zhu, F.S. Han, J. Banhart, Internal friction of foamed aluminium in the range of acoustic frequencies, Journal of Materials Science 33 (1998) 1769–1775.
[16] J. Zhang, M.N. Gungor, E.J. Lavernia, The effect of porosity on the microstructural damping response of 6061 aluminium alloy, Journal of Materials Science 28 (1993) 1515–1524.
[17] S.D. Panteliou, K. Zonios, I.T. Chondrou, H.R. Fernandes, S. Agathopoulos, J.M.F. Ferreira, Damping associated with porosity in alumina, International Journal of Mechanics and Materials Design 5 (2009) 167–174.
[18] B. Paul, Prediction of elastic constants of multiphase materials, Transactions on Metallurgical Society of AIME 218 (1960) 36–41.
[19] D.J. Green, An Introduction to the Mechanical Properties of Ceramics, Cambridge University Press, Cambridge/UK, 1998, pp. 78–94.
[20] W. Pabst, E. Gregorová, Effective elastic properties of alumina–zirconia composite ceramics – part I: rational continuum theory of linear elasticity, Ceramics – Silikaty 47 (2003) 1–7.
[21] W. Pabst, E. Gregorová, Effective elastic properties of alumina–zirconia composite ceramics – part II: micromechanical modeling, Ceramics – Silikaty 48 (2004) 14–23.
[22] Z. Hashin, S. Shtrikman, A variational approach to the theory of the elastic behaviour of multiphase materials, Journal of the Mechanics and Physics of Solids 11 (1963) 127–140.
[23] W. Pabst, E. Gregorová, Effective elastic moduli of alumina, zirconia and alumina–zirconia composites, in: B.M. Caruta (Ed.), Ceramics and Composite Materials, Nova Science Publishers, New York, 2006, pp. 31–100.
[24] W. Pabst, E. Gregorová, Note on the so-called Coble-Kingery formula for the effective tensile modulus of porous ceramics, Journal of Materials Science Letters 22 (2003) 959–962.
[25] W. Pabst, E. Gregorová, Derivation of the simplest exponential and power-law relations for the effective tensile modulus of porous ceramics via functional equations, Journal of Materials Science Letters 22 (2003) 1673–1675.
[26] W. Pabst, E. Gregorová, Mooney-type relation for the porosity dependence of the effective tensile modulus of ceramics, Journal of Materials Science 39 (2004) 3213–3215.
[27] W. Pabst, E. Gregorová, I. Sedlářová, M. Černý, Preparation and characterization of porous alumina–zirconia composite ceramics, Journal of the European Ceramic Society 31 (2011) 2721–2731.

[28] M. Černý, P. Glogar, L.M. Manocha, Resonant frequency study of tensile and shear elasticity moduli of carbon fibre reinforced composites (CFRC), Carbon 38 (2000) 2139–2149.
[29] M. Černý, P. Glogar, Young's modulus of ceramic matrix composites with polysiloxane based matrix at elevated temperatures, Journal of Materials Science 39 (2004) 2239–2242.
[30] M. Weller, H. Schubert, Internal friction, dielectric loss, and ionic conductivity of tetragonal ZrO_2–3% Y_2O_3 (Y-TZP), Journal of the American Ceramic Society 69 (1986) 573–577.
[31] E. Gregorová, W. Pabst, Porosity and pore size control in starch consolidation casting – achievements and problems, Journal of the European Ceramic Society 27 (2007) 669–672.
[32] E. Gregorová, Z. Živcová, W. Pabst, Starch as a pore-forming and body-forming agent in ceramic technology, Starch/Stärke 61 (2009) 495–502.
[33] E. Schreiber, O.L. Anderson, N. Soga, Elastic Constants and Their Measurement, McGraw-Hill, New York, 1973, pp. 82–125.
[34] R.M. German, Particle Packing Characteristics, Metal Powder Industries Federation, Princeton/NJ, 1989, pp. 67–177.
[35] J. Hostaša, Thermal conductivity of Al_2O_3/ZrO_2 composite ceramics (in Czech). M.Sc. Thesis, Institute of Chemical Technology, Prague (ICT Prague), Prague, 2010.
[36] D.J. Green, O. Guillon, J. Rödel, Constrained sintering: a delicate balance of scales, Journal of the European Ceramic Society 28 (2008) 1451–1466.
[37] W. Pabst, E. Gregorová, Effective thermal and thermoelastic properties of alumina, zirconia and alumina–zirconia composites, in: B.M. Caruta (Ed.), New Developments in Materials Science Research, Nova Science Publishers, New York, 2007, pp. 77–137.
[38] P. Pialy, N. Tessier-Doyen, D. Njopwouo, J.P. Bonnet, Effects of densification and mullitization on the evolution of the elastic properties of a clay-based material during firing, Journal of the European Ceramic Society 29 (2009) 1579–1586.
[39] S. Deniel, N. Tessier-Doyen, C. Dublanche-Tixier, D. Chateigner, P. Blanchart, Processing and characterization of textured mullite ceramics from phyllosilicates, Journal of the European Ceramic Society 30 (2010) 2427–2434.
[40] W. Pabst, E. Gregorová, G. Tichá, Elasticity of porous ceramics – a critical study of modulus–porosity relations, Journal of the European Ceramic Society 26 (2006) 1085–1097.
[41] Z. Živcová, M. Černý, W. Pabst, E. Gregorová, Elastic properties of porous oxide ceramics prepared using starch as a pore-forming agent, Journal of the European Ceramic Society 29 (2009) 2765–2771.
[42] W.H. Tuan, R.Z. Chen, T.C. Wang, C.H. Cheng, P.S. Kuo, Mechanical properties of Al_2O_3/ZrO_2 composites, Journal of the European Ceramic Society 22 (2002) 2827–2833.
[43] S.R. Choi, N.P. Bansal, Mechanical behavior of zirconia/alumina composites, Ceramics International 31 (2005) 39–46.
[44] M. Chmelíčková, Preparation and characterization of oxide ceramics with porous microstructure (in Czech). M.Sc. Thesis, Institute of Chemical Technology, Prague (ICT Prague), Prague, 2010.
[45] W. Pabst, E. Gregorová, G. Tichá, E. Týnová, Effective elastic properties of alumina–zirconia composite ceramics – part IV: tensile modulus of porous alumina and zirconia, Ceramics – Silikaty 48 (2004) 145–153.
[46] Z. Živcová, Preparation and characterization of porous oxide ceramics (in Czech). Ph.D. Thesis, Institute of Chemical Technology, Prague (ICT Prague), Prague, 2010.
[47] W. Pabst, G. Tichá, E. Gregorová, E. Týnová, Effective elastic properties of alumina–zirconia composite ceramics – partV: tensile modulus of alumina–zirconia composite ceramics, Ceramics – Silikaty 49 (2005) 77–85.